Code Range and Carrier Phase Multipath Mitigation Using SNR, Range and Phase Measurements in a Multi-Antenna System

J.K. Ray
M.E. Cannon
Department of Geomatics Engineering
University of Calgary

P. Fenton
NovAtel Inc.

BIOGRAPHY

Jayanta Kumar Ray is a Ph.D. student in Geomatics Engineering at the University of Calgary. He received a B.E. and M.Tech. in Electronics Engineering from the Bangalore University and Indian Institute of Science, India, respectively. He has been involved in GPS research since 1992 in the area of GPS receiver hardware and software development and the mitigation of multipath.

M. Elizabeth Cannon is Professor of Geomatics Engineering at the University of Calgary. She has been involved in GPS research and development since 1984, and has worked extensively on the integration of GPS and inertial navigation systems for precise aircraft positioning. Dr. Cannon is a Past President of the ION.

Patrick C. Fenton is the Vice President of Research and Development at Novatel. He received B.Sc. in Surveying Engineering from the University of Calgary in 1981. He worked at Nortech Surveys developing specialized survey equipment including INS/GPS and Laser primarily for oil exploration applications. In 1989 he joined NovAtel to lead the technical development of their GPS receivers. He was the inventor of NovAtel's Narrow Correlator technology.

ABSTRACT

Multipath is a major source of error in high precision GPS static and kinematic differential positioning. It is a major concern in reference stations such as in Local Area Augmentation Systems (LAAS), whereby corrections generated by a reference station which are based on multipath corrupted measurements, can significantly influence the position accuracy of differential users. Code range, carrier phase and signal-to-noise (SNR) measurements are all affected by multipath, and is spatially correlated within a small area. In order to estimate and remove code and carrier phase multipath, a system comprising of a cluster of five GPS receivers and antennas is used at a reference station location. The spatial correlation of the receiver data, and the known geometry among the antennas, are exploited to estimate multipath for each satellite in each antenna in the system. The paper analyzes generic receiver code and carrier tracking loop discriminator functions, and formulates relationships between receiver data, such as code range, carrier phase and SNR measurements and relates them to various multipath parameters. A Kalman filter is described which uses a combination of the available information from the antennas (receivers) in the multi-antenna cluster to estimate various multipath parameters. From the multipath parameters, the code range and carrier phase multipath is estimated and compensated. The technique is first tested on simulated data in a controlled multipath environment. Results are then presented using field data and show a significant reduction in multipath error.

INTRODUCTION

An important aspect of a Local Area Augmentation System (LAAS) is to provide carrier smoothed range corrections to an aircraft to reduce residual range errors (Decleene et al., 1997). The current RTCA proposal is to use a smoothing time constant of 100 seconds, but one of the major problems of achieving high accuracy ranges, and thereby high accuracy positions in differential mode, is multipath. Distant reflectors cause high frequency code multipath which can be mitigated by some currently available special correlator techniques, e.g. Narrow Correlator^{TM} (van Dierendonck et al., 1992), Multipath Elimination Technique (MET^{TM}) (Townsend and Fenton, 1994), MEDLL^{TM} (van Nee, 1995), Edge Correlator^{TM} technique (Garin et al., 1996), Strobe Correlator^{TM} and Enhanced Strobe Correlator^{TM} (Garin and Rousseau, 1997). Similarly, high frequency carrier multipath can be mitigated by MEDLL^{TM} (Townsend et al., 1995) and the Enhanced Strobe Correlator^{TM} (Garin and Rousseau, 1997). Furthermore, high frequency code multipath is

substantially reduced by using a carrier smoothing technique (Hatch, 1982).

Low frequency multipath due to close-by reflectors is still a problem for most currently available correlator-based techniques, and therefore cannot be reduced effectively by carrier smoothing. Special antennas, which have a sharp cutoff below certain elevation angles, have also been employed for multipath reduction (Counselman, 1998; Bartone and van Graas, 1998), however multipath arriving at high elevation angles due to reflection from tall buildings and structures will still not be eliminated.

This paper describes a method which uses a system comprised of a cluster of five GPS receivers and antennas to estimate and mitigate code and carrier multipath errors using any or all of code range, carrier phase and SNR information from a receiver. The spatial correlation of these measurements, and the known geometry among the antennas, are exploited to estimate multipath for each satellite in each antenna in the system. Generic receiver code and carrier tracking loop discriminator functions are analyzed and relationships between the code, carrier phase and SNR measurements are formulated to relate them to various multipath parameters.

This overall objective is to demonstrate that the code, carrier phase and SNR data can be used in an antenna cluster configuration to mitigate multipath. This work is an extension of that given in Ray et al. (1998) and Ray (1999). The technique is first tested on simulated data in a controlled multipath environment. Results are then presented using field data and show a significant reduction in multipath error.

RECEIVER TRACKING LOOPS

Figure 1 shows a block diagram of a typical receiver's tracking loops, which consists of a Delay Lock Loop (DLL) for code tracking and a Costas Loop for carrier tracking (Ward, 1996; GEC Plessey, 1996). The DLL has a non-coherent type of discriminator. An *n* parallel channel receiver will have *n* such sets of blocks corresponding to each independent tracking loop. In a receiver, the digitized IF signal is input to each of these parallel channels. The input signal is beat with a locally generated in-phase and quadrature phase replica of the carrier. The signal is then correlated with the prompt, early and late versions of the locally generated code, and the correlation values are integrated for a pre-detection integration period. The early and late correlation values in the in-phase and quadrature arms are generally used for code tracking, whereas the prompt correlation values are used for carrier tracking. Some code discriminators, such as the dot-product type, use prompt correlation values as well. For analysis of the effects of multipath on GPS code and carrier measurements, the code and carrier discriminator function characteristics in the presence of multipath need to be analyzed.

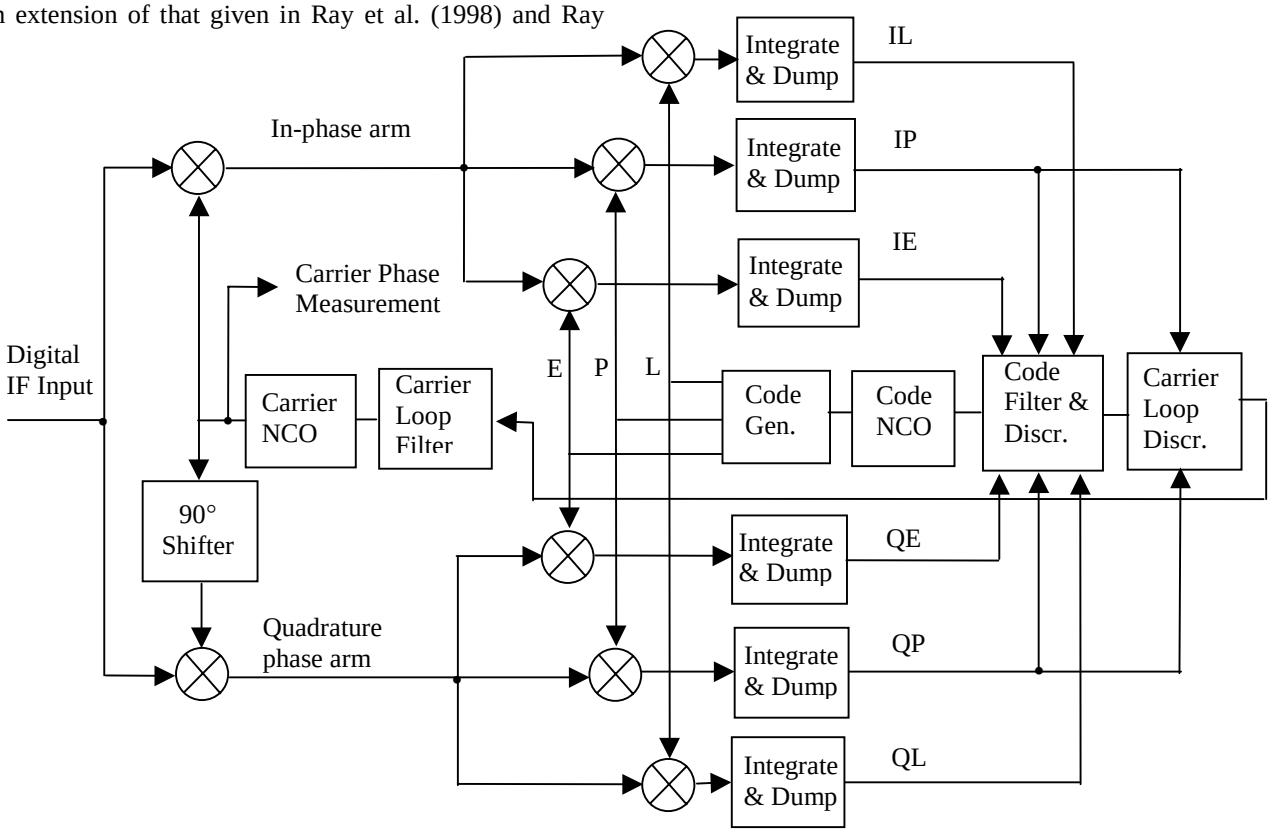

Figure 1: Typical GPS receiver code and carrier tracking loops (Ward, 1996; GEC Plessey, 1996)

A GPS receiver may receive a number of reflected signals along with the direct signal from the satellite. The composite input signal, neglecting the navigation data bit, can be expressed as

$$s(t)=c(t)A\sum_{i=0}^{n}\alpha_i\cos(\omega_0 t+\gamma_i) \quad (1)$$

where,

- c(t) is the GPS C/A or P code,
- A is the carrier signal amplitude,
- α_i are the direct and reflected signal coefficient (where α_0 corresponds to direct signal and equal to 1),
- ω_0 is the satellite signal frequency (rad/sec), and
- γ_i is the phase of the *i*th signal (rad).

The in-phase early correlation value, assuming that the incoming and the locally generated carrier frequencies are the same, is given as

$$IE=\sum_{0}^{N}\sum_{0}^{n}\alpha_i\frac{A}{2}R(\hat{\tau}_c-\tau_i+T_d)\cos(\gamma_i-\hat{\gamma}_c) \quad (2a)$$

where,

- N is the number of samples in the pre-detection integration period,
- R() is the correlation function,
- $\hat{\tau}_c$ is the receiver's estimate of the incoming signal code delay (m),
- T_d is the spacing of early or late correlator with respect to the prompt correlator (m), and
- $\hat{\gamma}_c$ is the receiver's estimate of the incoming signal carrier phase (rad).

Similarly, the in-phase late (IL), in-phase prompt (IP), quadrature phase early (QE), quadrature phase late (QL), and quadrature phase prompt (QP) correlation values in the presence of multipath are respectively,

$$IL=\sum_{0}^{N}\sum_{0}^{n}\alpha_i\frac{A}{2}R(\hat{\tau}_c-\tau_i-T_d)\cos(\gamma_i-\hat{\gamma}_c)$$

$$IP=\sum_{0}^{N}\sum_{0}^{n}\alpha_i\frac{A}{2}R(\hat{\tau}_c-\tau_i)\cos(\gamma_i-\hat{\gamma}_c)$$

$$QE=\sum_{0}^{N}\sum_{0}^{n}\alpha_i\frac{A}{2}R(\hat{\tau}_c-\tau_i+T_d)\sin(\gamma_i-\hat{\gamma}_c) \quad (2b\text{-}2f)$$

$$QL=\sum_{0}^{N}\sum_{0}^{n}\alpha_i\frac{A}{2}R(\hat{\tau}_c-\tau_i-T_d)\sin(\gamma_i-\hat{\gamma}_c)$$

$$QP=\sum_{0}^{N}\sum_{0}^{n}\alpha_i\frac{A}{2}R(\hat{\tau}_c-\tau_i)\sin(\gamma_i-\hat{\gamma}_c)$$

These correlation values are used by code and carrier discriminator functions for continuous code and carrier tracking, respectively.

MULTIPATH EFFECT ON THE CODE RANGE

Various types of coherent and non-coherent discriminator functions are employed for code tracking. The following analysis is carried out for a non-coherent dot-product type of discriminator as subsequent analysis with field data was done with a receiver employing this type of discriminator. Similar analyses were done for typical coherent and non-coherent types of discriminators as well, but are not discussed below.

A dot-product type of discriminator is given by (Ward, 1996)

$$D_n = IP(IE-IL)+QP(QE-QL) \quad (3)$$

For continuous tracking, D_n is equated to zero and the resultant delay error is computed and input to the code loop filter for generating correction to the code NCO.

For this discriminator, the multipath due to a single dominant reflector, or a virtual reflector which is the mathematical equivalent of a combination of physical reflectors (Ray et al., 1998), can be determined from equations (2) and (3) and is given by,

$$\begin{aligned} D_n = &\left\{R(\hat{\tau}_c-\tau_0)+R(\hat{\tau}_c-\tau_1)\right\}\\ &\left\{R(\hat{\tau}_c-\tau_0+T_d)+R(\hat{\tau}_c-\tau_1-T_d)\right\}+\\ &\left\{\begin{array}{l}\alpha R(\hat{\tau}_c-\tau_0)\left[\begin{array}{l}R(\hat{\tau}_c-\tau_0+T_d)-\\R(\hat{\tau}_c-\tau_1-T_d)\end{array}\right]+\\ \alpha R(\hat{\tau}_c-\tau_1)\left[\begin{array}{l}R(\hat{\tau}_c-\tau_0+T_d)-\\R(\hat{\tau}_c-\tau_1-T_d)\end{array}\right]\end{array}\right\}\cos(\gamma_0-\gamma_1) \quad (4)\\ &=0 \end{aligned}$$

Equation (4) does not have the term $\hat{\gamma}_c$, which means that code tracking does not depend on carrier phase tracking as long as the carrier frequency is locked. Multipath error can be computed by assuming that $\tau_0 = 0$ and then $\hat{\tau}_c$ is the multipath error.

As mentioned earlier, multipath from nearby reflectors (τ_1 < 30 m for the C/A code) is a major problem with most of the currently available receivers as correlator-based mitigation techniques remove multipath due to distant reflectors. Therefore, for nearby reflectors ($0<\tau_1<(1+\alpha)T_d$), assuming the multipath error is much smaller than the chip width and path delay, and by

substituting the correlation symbol 'R' by its values in equation (4), the code multipath error is given by,

$$\hat{\tau}_c = \frac{\alpha T(1-\alpha')\cos\gamma}{1+\alpha'+\alpha\cos\gamma+\alpha\alpha'\cos\gamma} = T\left(\frac{1-\alpha'}{1+\alpha'}\right)\left(\frac{\alpha\cos\gamma}{1+\alpha\cos\gamma}\right) \quad (5)$$

where,

α' is the correlation ratio and is given by

$$\frac{R(\hat{\tau}_c-\tau_1)}{R(\hat{\tau}_c)} = \frac{1-\left|\frac{\hat{\tau}_c-\tau_1}{T}\right|}{1-\left|\frac{\hat{\tau}_c}{T}\right|} \approx \frac{T-\tau_1}{T} \quad (6)$$

T is the chip width (m), and

γ is the reflected signal relative phase with respect to the direct signal and equal to γ_0-γ_1 (rad).

Multipath error is spatially correlated as shown in Ray et al. (1998) and Ray and Cannon (1999). Therefore, if several antennas are placed close-by, then multipath experienced by each of the antennas will be correlated, provided the reflector is large enough compared to the largest spacing between the antennas. The difference in code multipath error at two closely-spaced antennas, assuming the reflected signal strength is the same at both the antennas, is then given by,

$$\Delta\tau_c = \hat{\tau}_{c0} - \hat{\tau}_{ci} = T\left(\frac{1-\alpha'}{1+\alpha'}\right)\left(\frac{\alpha\cos\gamma_1-\alpha\cos\gamma_2}{1+\alpha\cos\gamma_1+\alpha\cos\gamma_2+\alpha^2\cos\gamma_1\cos\gamma_2}\right) \quad (7)$$

where,

γ_0 is reflected signal relative phase at antenna 0, and

γ_i is reflected signal relative phase at antenna i.

Equation (7) relates the code range multipath error at two closely-spaced antennas in terms of the reflection coefficient, correlation ratio and reflected signal phases. This relationship is exploited in the subsequent section to estimate multipath errors at each antenna.

MULTIPATH EFFECT ON THE CARRIER PHASE

In a Frequency Lock Loop (FLL), the local carrier frequency closely follows the incoming carrier frequency, but in a Phase Lock Loop, such as a Costas Loop, the local carrier phase closely follows the incoming carrier phase (Ward 1996). However, as the incoming signal may consist of the direct signal and many multipath signals, the local carrier follows the composite signal and the difference between the composite signal and the direct signal is the multipath error. It is given by (Braasch, 1996; Ray et al., 1998)

$$\Delta\Psi = \arctan\left(\frac{R(\tau-\tau_1)\alpha\sin\gamma}{R(\tau)+R(\tau-\tau_1)\alpha\cos\gamma}\right) = \arctan\left(\frac{\alpha\alpha'\sin\gamma}{1+\alpha\alpha'\cos\gamma}\right) \quad (8)$$

It is interesting to note that when multipath is due to close-by ($\alpha' \approx 1$) and weak ($\alpha << 1$) reflectors, then from equations (5) and (8), the code and carrier multipath errors have similar, but phase shifted, patterns. In general, both types of multipath are related to various multipath parameters and correlation ratios in definite but different ways. This also means that code and carrier multipath errors are closely related to each other and the error frequency is determined by the multipath phase rate in both cases. This brings out a synergistic relationship between the two types of multipath.

The difference in carrier multipath error at two closely-spaced antennas, assuming the reflected signal strength is the same at both the antennas, is then given by,

$$\Delta\Psi_{0,i} = \Delta\Psi_0 - \Delta\Psi_i = \arctan\left(\frac{\alpha\alpha'\sin\gamma_0-\alpha\alpha'\sin\gamma_i+\alpha^2\alpha'^2\sin(\gamma_0-\gamma_i)}{1+\alpha\alpha'\cos\gamma_0-\alpha\alpha'\cos\gamma_i+\alpha^2\alpha'^2\cos(\gamma_0-\gamma_i)}\right) \quad (9)$$

Equation (9) relates the carrier phase multipath error at two closely-spaced antennas in terms of reflection coefficient, correlation ratio and reflected signal phases. This relationship is exploited in the subsequent section to estimate multipath errors at each antenna.

MULTIPATH EFFECT ON THE SNR

A GPS signal is transmitted from the satellite through a shaped pattern antenna array to compensate for the increased path loss to the users at low elevation angles (Spilker, 1996). Another element that affects the signal power at the receiver is the antenna gain pattern. The antenna gain pattern in reality may be quite different from its ideal shape due to the effect of the ground plane, nearby large metal structures or proximity to other antennas.

Multipath affects not only the code range and carrier phase measurements, but also the measured signal power, which is an average of the composite signal power due to the direct and reflected signal carrier. As the reflected signal relative phase varies with time, the power of the composite signal also varies with time and so does the measured power, commonly expressed as C/N_0.

However, estimating multipath from SNR in a receiver poses several problems, especially if real time application is the objective. In post processing, one can find the frequency components of the SNR by a Fast Fourier Transform (FFT) or other suitable frequency resolution techniques and reconstruct the multipath error from the frequency and phase of the dominant components. This was demonstrated by Axelrad et al. (1996).

The relationship between the SNR and multipath parameters is given in Ray and Cannon (1999). Assuming a uniform antenna gain pattern, the average received signal power can be easily calculated, and is given by,

$$P = P_0\left(1 + \alpha^2\alpha'^2 + 2\alpha\alpha'\cos\gamma\right) \tag{10}$$

where P_0 is the average power of the direct carrier signal and is equal to $\frac{A^2}{2}$.

In a receiver, the signal power is generally measured using the following equation

$$P = IP^2 + IQ^2 \tag{11}$$

By replacing the values of IP and IQ from equation (2), equation (10) can be obtained. From equation (10), the average signal power in the receiver is a function of the reflection coefficient, correlation ratio and the relative phase of the reflected signal.

The SNR error in multiple closely-spaced antennas are correlated, though the nature of correlation is not the same as for the code and carrier. This is because the code, carrier and SNR errors are related to the multipath parameters through a different relationship. The correlation of SNR error among the antennas may be exploited to estimate multipath parameters. By differencing the SNR between antennas, and by carefully arranging the antennas in the assembly, it is possible to reduce the problem of variation in the SNR due to elevation as well as antenna gain pattern modeling.

Assuming that the noise power spectral density is the same for two closely-spaced antennas, the ratio of the SNR between two antennas is given by,

$$R_{0,i} = \frac{P_i/N_i}{P_0/N_0} = \frac{\left(1 + \alpha^2\alpha'^2 + 2\alpha\alpha'^2\cos\gamma_i\right)}{\left(1 + \alpha^2\alpha'^2 + 2\alpha\alpha'\cos\gamma_0\right)} \tag{12}$$

Equation (12) relates the ratio of the SNRs at two closely-spaced antennas in terms of the reflection coefficient, correlation ratio and reflected signal phases. This relationship is exploited in the subsequent section to estimate multipath parameters and thereby multipath errors at each antenna.

MULTIPATH PARAMETER ESTIMATOR

Assuming that the correlation ratio and reflection coefficient are the same for each antenna, and that the antenna gain pattern of the antennas is identical, then the multipath error at each antenna depends only on the reflected signal relative phase. The reflected signal phase at one antenna phase center with respect to the phase at another antenna phase center in a closely-spaced antenna cluster in the horizontal plane is given by

$$\gamma_i = \gamma_0 + \frac{2\pi}{\lambda} a_{0i}\cos(\varphi_0 - \phi_{0i})\cos\theta_0 \tag{13}$$

where,

- λ is the carrier wavelength (m),
- a_{0i} is the distance between antennas 0 and i (m),
- ϕ_{0i} is the azimuth of the vector from antenna 0 to i (rad),
- θ_0 is the elevation of the reflected signal (rad), and
- φ_0 is the azimuth of the reflected signal (rad).

To determine the relative phase at each antenna using this equation, the difference in range due to the spatial separation between the two antennas needs to be compensated.

In equations (7), (9) and (12), the multipath error on code, carrier and SNR in two closely-spaced antennas due to a virtual reflector is related to various multipath parameters. Similar equations can be derived for different sets of antenna pairs. Therefore, for a cluster of *m* closely-spaced antennas, there will be (*m*-1) such equations. Assuming that the reflection coefficient and correlation ratio are the same for all antennas, there will be (*m*+1) unknown parameters (one reflection coefficient, one correlation ratio and (*m*-1) reflected signal relative phases). By using equation (13), it is possible to relate the (*m*-1) reflected signal relative phases in terms of three unknown parameters, namely the reflected signal relative phase at one antenna (known as the reference antenna), the azimuth and the elevation angle of the reflected signal. Therefore, there are a total of five unknown parameters.

An Extended Kalman Filter (Gelb, 1979; Maybeck, 1994) was developed with the above parameters as state variables, i.e.

$$\begin{bmatrix} \alpha \\ \alpha' \\ \gamma_0 \\ \theta_0 \\ \varphi_0 \end{bmatrix} = \begin{bmatrix} \text{Reflection coefficient} \\ \text{Correlation ratio} \\ \text{Reflected signal relative phase at the ref ant} \\ \text{Reflected signal elevation} \\ \text{Reflected signal azimuth} \end{bmatrix} \tag{14}$$

Single difference (between antenna) code range and carrier phase measurements are used to update the state variables as well as SNR ratios.

The single difference code and carrier phase are free from atmospheric delay errors, satellite orbital errors, and satellite clock errors, and are given by the following (Lachapelle, 1997)

$$\begin{aligned}\Delta P_{0i} &= \Delta\rho_{0i} + c\Delta t_{0i} + \Delta\varepsilon_{p0i} + \Delta\varepsilon_{Mp0i} \\ \Delta\Phi_{0i} &= \Delta\rho_{0i} + c\Delta t_{0i} + \Delta N_{0i}\lambda + \Delta\varepsilon_{\varphi 0i} + \Delta\varepsilon_{M\varphi 0i}\end{aligned} \quad (15)$$

where,

- ΔP is the measured code range single difference between antennas (m),
- $\Delta\Phi$ is the measured carrier phase single difference between antennas (m),
- $\Delta\rho$ is the range difference due to spatial separation between antennas (m),
- $c\Delta t$ is the receiver clock bias difference (m),
- ΔN is the integer ambiguity difference (cycles),
- $\Delta\varepsilon_P$ is the receiver code noise difference (m),
- $\Delta\varepsilon_\varphi$ is the carrier phase noise difference (m),
- $\Delta\varepsilon_{Mp}$ is the code range multipath error difference (m), and
- $\Delta\varepsilon_{M\varphi}$ is the carrier phase multipath error difference (m).

Each antenna in the multi-antenna system is connected to a different receiver. If the receivers are driven by a common clock, and their code range measurements and carrier phase measurements are corrected for the antennas' spatial separations, then the single difference code range measurements contain only the single difference code multipath error and receiver code noise. Similarly, single difference carrier phase measurements contain only the difference of the integer ambiguity, single difference carrier multipath and phase noise. As the multipath and phase noise together are much smaller compared to the carrier wavelength, the integer cycles can be easily removed and the resultant modified single difference contains only the difference of multipath and phase noise between the antennas. Neglecting receiver code noise and phase noise gives,

$$\begin{aligned}\Delta\tau_{0i} &= \Delta P_{0i} \\ \Delta\Psi_{0i} &= \Delta\Phi_{0i}\end{aligned} \quad (16)$$

If C_0 and C_i are the carrier to noise power spectral densities (C/N_0) of a satellite signal at two closely-spaced antennas, assuming the noise spectral density of the two receivers to be the same, then

$$R_{0i} = \frac{Pi}{P_0} = 10^{\frac{(C_i - C_0)}{10}} \quad (17)$$

Therefore, in *m* closely-spaced antennas, if one of the antennas in the (*m*-1) antenna pairs is common, then the number of measurements would be (*m*-1) single difference code range measurements, (*m*-1) single difference carrier phase measurements and (*m*-1) ratios of the SNRs. Therefore,

$$z = \left[\Delta\tau_{0,1} \,..\, \Delta\tau_{0,m-1} \;\; \Delta\Psi_{0,1} \,..\, \Delta\Psi_{0,m-1} \;\; R_{0,1} \,..\, R_{0,m-1}\right]^T \quad (18)$$

The relationship between the state variables and the measurements is contained in the design matrix. As the relationship is non-linear in nature, it is obtained by substituting equation (13) into equations (7), (9) and (12), and then computing the partial derivatives with respect to the unknown parameters. The resulting design matrix is

$$\begin{bmatrix}
\frac{\delta(\tau_{0,1})}{\delta\alpha} & \frac{\delta(\tau_{0,1})}{\delta\alpha'} & \frac{\delta(\tau_{0,1})}{\delta\gamma_0} & \frac{\delta(\tau_{0,1})}{\delta\theta_0} & \frac{\delta(\tau_{0,1})}{\delta\varphi_0} \\
--- & --- & --- & --- & --- \\
\frac{\delta(\tau_{0,m-1})}{\delta\alpha} & \frac{\delta(\tau_{0,m-1})}{\delta\alpha'} & \frac{\delta(\tau_{0,m-1})}{\delta\gamma_0} & \frac{\delta(\tau_{0,m-1})}{\delta\theta_0} & \frac{\delta(\tau_{0,m-1})}{\delta\varphi_0} \\
\frac{\delta(\Psi_{0,1})}{\delta\alpha} & \frac{\delta(\Psi_{0,1})}{\delta\alpha'} & \frac{\delta(\Psi_{0,1})}{\delta\gamma_0} & \frac{\delta(\Psi_{0,1})}{\delta\theta_0} & \frac{\delta(\Psi_{0,1})}{\delta\varphi_0} \\
--- & --- & --- & --- & --- \\
\frac{\delta(\Psi_{0,m-1})}{\delta\alpha} & \frac{\delta(\Psi_{0,m-1})}{\delta\alpha'} & \frac{\delta(\Psi_{0,m-1})}{\delta\gamma_0} & \frac{\delta(\Psi_{0,m-1})}{\delta\theta_0} & \frac{\delta(\Psi_{0,m-1})}{\delta\varphi_0} \\
\frac{\delta(R_{0,1})}{\delta\alpha} & \frac{\delta(R_{0,1})}{\delta\alpha'} & \frac{\delta(R_{0,1})}{\delta\gamma_0} & \frac{\delta(R_{0,1})}{\delta\theta_0} & \frac{\delta(R_{0,1})}{\delta\varphi_0} \\
--- & --- & --- & --- & --- \\
\frac{\delta(R_{0,m-1})}{\delta\alpha} & \frac{\delta(R_{0,m-1})}{\delta\alpha'} & \frac{\delta(R_{0,m-1})}{\delta\gamma_0} & \frac{\delta(R_{0,m-1})}{\delta\theta_0} & \frac{\delta(R_{0,m-1})}{\delta\varphi_0}
\end{bmatrix} \quad (19)$$

In the Kalman filter, the state variables are described as simple first order Gauss-Markov processes (Gelb, 1979; Maybeck, 1994). The correlation time was selected to be about 1 minute and an appropriate process noise was chosen for each of the state variables. Selection of the process noise plays a crucial role in the estimation, as the filter is quite sensitive to this value.

The above filter is used to estimate the unknown parameters for a particular satellite. As the filter estimates the parameter based on the measurements that are affected by multipath from all sources in the environment, the estimates refer to the composite multipath. After the parameters are estimated, the multipath error can be easily estimated by using equations (5) and (8). This technique has to be repeated for each satellite, or alternatively parallel independent filters are to be used for each satellite.

The above formulation is quite generic in nature and includes code, carrier and SNR information. However, it is possible to estimate the multipath parameters from a subset of the information. For example, in principle, it is possible to estimate multipath parameters from either code, carrier, or SNR information alone, or a combination of two can also be used, as long as there are at least as many observations as unknown parameters.

Another point to be highlighted is that the correlation ratio parameter appears separately in the derivation of the code multipath formulation, but it appears simultaneously with the reflection coefficient in the carrier multipath and SNR formulation. Therefore, to determine carrier phase multipath error, these two parameters may be combined together to give a single parameter such as a modified reflection coefficient. Even for code multipath, it is possible to fix the value of the correlation ratio to a constant and therefore estimate the other four parameters. In this case however, the other parameters will absorb the influence of the time variation of the correlation ratio.

TEST DESCRIPTION

The proposed multipath mitigation technique was tested using the Multipath Simulation and Mitigation (MultiSim) software (Ray and Cannon, 1999). After having successfully demonstrated the mitigation of multipath using the above model on simulated multipath, the same approach was applied to field data as discussed below.

A special antenna array was assembled whereby a thick aluminum plate was used to rigidly mount six antennas close together. NovAtel Model 521 antennas were used, as they are small with a diameter of approximately 5.6 cm.

NovAtel BeeLine™ receivers were used for data collection (Ford et al., 1997), wherein all receivers were driven by the same external rubidium oscillator. The antenna assembly was placed on a surveyed pillar (on the roof of the Engineering Building) where there are concrete sidewalls of approximately 3 m in height on the east side and 1 meter in height on the south side which are expected to cause low frequency multipath errors.

The antenna array was used as a reference receiver for the tests. A NovAtel Millennium™ receiver with a choke ring antenna (user) was placed in an open field where there were no major objects in the range of 80 to 100 m from the antenna. The baseline separation from the antenna array to the MiLLennium™ was approximately 500 m. Only L1 data from the MiLLennium™ was used.

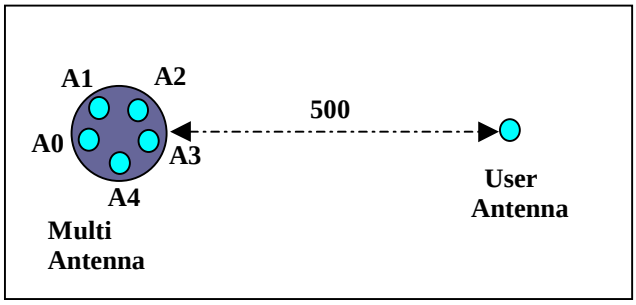

Figure 2: Experimental setup

Field trials were conducted on October 20, 1998, whereby raw L1 carrier phase data was collected at 1 Hz. Antenna positions in the multi-antenna assembly were accurately surveyed to determine the inter-antenna vectors, and hence the relative geometry. The University of Calgary's Semikin™ software (Cannon, 1993) was used for this purpose.

The collected data was pre-processed and single difference code measurements (between antennas) for each satellite were computed. They were input to the Kalman filter, which estimated the multipath parameters. These parameters were then used to compute the code multipath error for each satellite at all antennas.

TEST RESULTS

Simulated Multipath Estimation

MultiSim (Ray and Cannon, 1999) was used to simulate a reflector in the vicinity of an antenna assembly at a desired location and stored ephemeris data was used to simulate satellite dynamics. The effect of multipath due to the reflector on the receiver code and carrier tracking loops for a particular type of discriminator function were computed, and multipath corrupted code, carrier and SNR measurements were generated. Figures 3, 4 and 5 show the simulated 'true' code, carrier and SNR multipath error due to a reflector, with a reflection coefficient of 0.5, placed 6 m away from the antenna assembly.

Single difference (between antenna) multipath-corrupted code, carrier and SNR measurements were input to the Kalman filter and the estimated multipath parameters are shown in Figure 6. In this case, the correlation ratio was held to a fixed value and as a result, its variation was absorbed by other parameters. The residuals of the measurements were very close to zero.

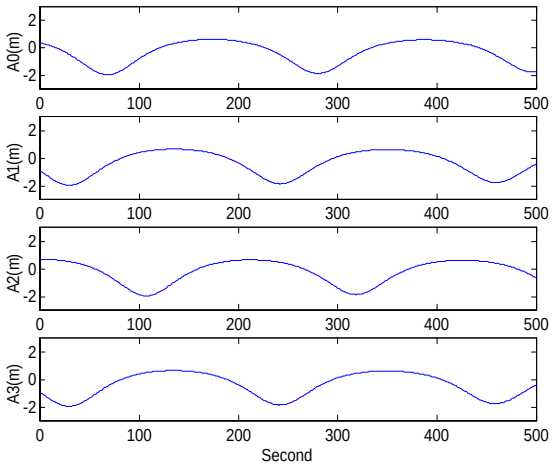

Figure 3: True code multipath error in reference antennas A0 to A3

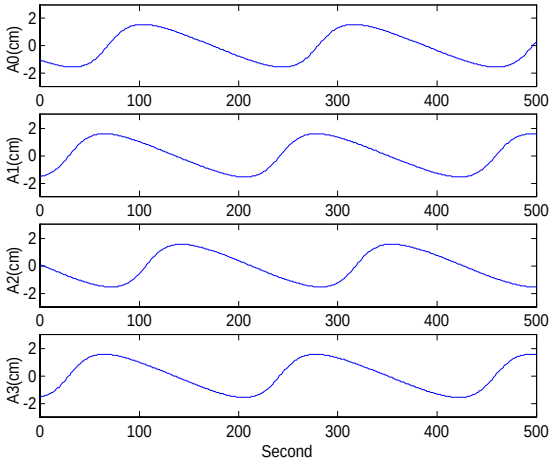

Figure 4: True carrier multipath error in reference antennas A0 to A3

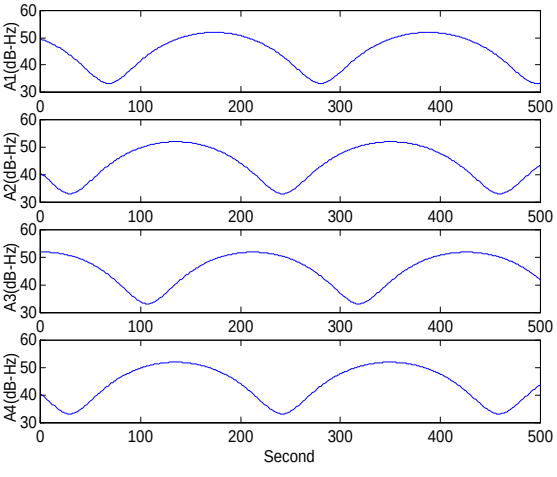

Figure 5: True SNR errors in reference antennas A0 to A3

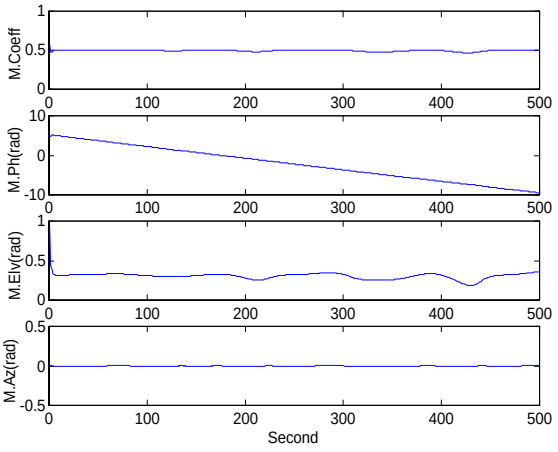

Figure 6: Estimated multipath parameters using code, carrier phase and SNR measurements

Multipath code and carrier error was computed from the estimated parameters and compared with their true values. Figures 7 and 8 show the difference between the true and computed code and carrier multipath, respectively. As can be seen, the computed multipath is very close to the true multipath and the resultant error in estimation is nearly zero. Simulations were carried out for various scenarios of antenna reflector geometry with different reflection coefficients, and similar results were obtained in all cases. This proves the correctness of the underlying theory of this technique.

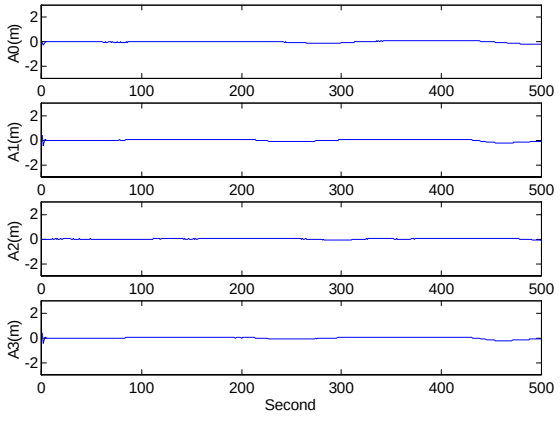

Figure 7: The difference between the true and estimated code multipath for antennas A0 to A3

Field Test Results

Code, carrier phase and SNR information from the antenna assembly were used to form single difference measurements, however it was found that the assumption that the noise power spectral density (N_0) would be the same for all the receivers was not valid. This is likely due to differences in the electrical characteristics of the various electronics components along the signal path in each receiver.

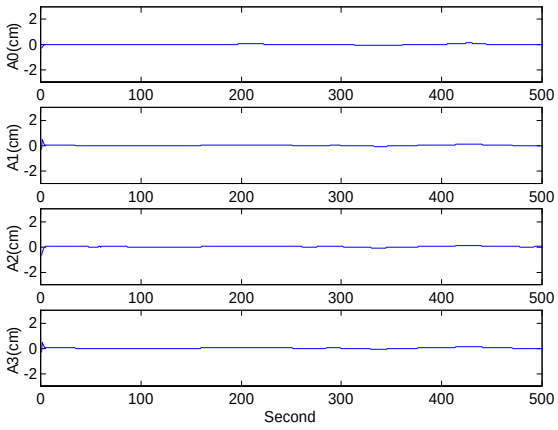

Figure 8: The difference between the true and estimated carrier multipath for antennas A0 to A3

Figure 9 shows the SNRs for various reference receivers for satellite 23, which has the highest elevation (71°-87°) during the test period. Figure 10 shows the same plots smoothed using a moving window of 500 seconds to remove errors due to multipath. From these figures it can be observed that each receiver has a different noise level, which varies with time and does not get canceled as previously assumed. Due to this problem, SNR measurements were not used when processing the field test data.

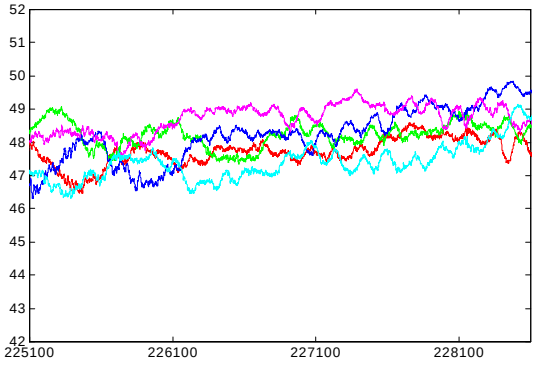

Figure 9: SNR at all the reference receivers for SV 23

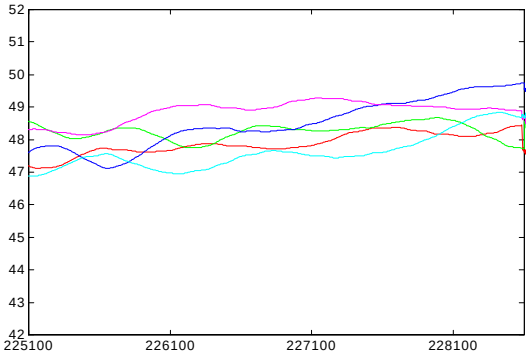

Figure 10: SNR at all the reference receivers for SV 23 averaged over a moving window of 500 seconds.

Appropriate weights were given to the code and carrier measurements and the multipath parameters were estimated. The residuals were found to be quite high and the computed code and carrier multipath were quite different from their measured values. Further investigations revealed that in the proposed model, code multipath was estimated for only close-by reflectors (i.e. multipath delay less than 30 meters for C/A code), whereas carrier phase multipath was estimated for all reflectors in the environment. Because of this discrepancy, the multipath parameters were not consistent between the two measurements. A simulation was carried out with a distant reflector, and as expected, the estimated parameters from both the code and carrier measurements were not correct, as were the computed multipath errors.

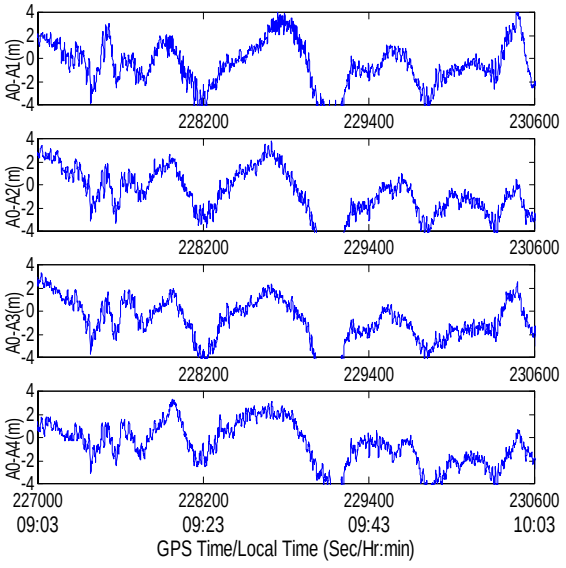

Figure 11: Single difference code measurements for SV 9 on October 20, 1998 (A0-A*n* denotes single difference between antennas 0 and *n*).

To overcome this problem, only code measurements were used for multipath parameter estimation. Figure 11 shows the single difference code measurements for satellite 1 where it can be seen that the multipath error is correlated among the reference antennas. Figure 12 gives the estimated parameters using the filter. The residuals in this case were not white and contained high frequency oscillations. This was because the proposed formulation did not model high frequency multipath as previously discussed.

Figure 13 shows the computed multipath error from the estimated parameters in a shaded dark line (blue) and the measured multipath in a shaded light line (green). As can be seen, the computed multipath closely follows the measured multipath error.

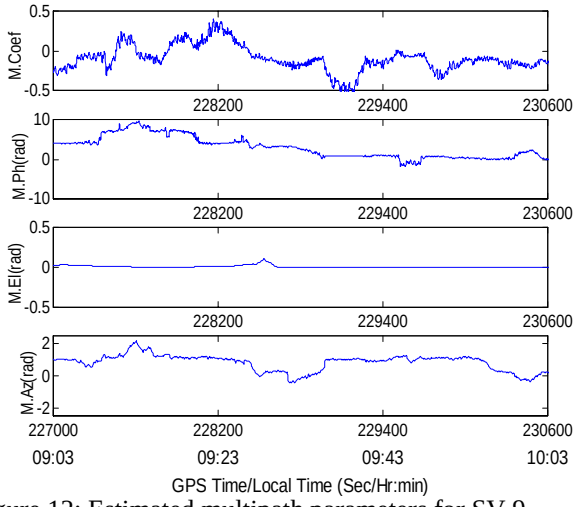

Figure 12: Estimated multipath parameters for SV 9

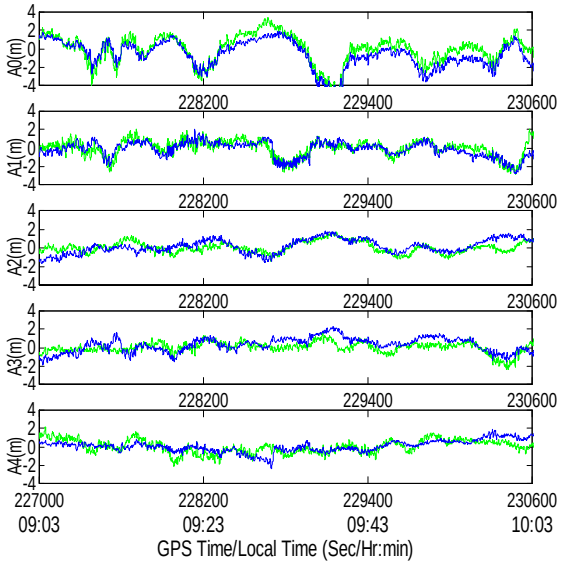

Figure 13: Measured multipath (light shade) and estimated multipath (dark shade) for SV 9. (A0…A*n* denote reference antennas 0…*n*).

Figure 14 shows the computed multipath errors for low elevation satellites, namely satellites 1, 9, 17 and 31 in a shaded dark line and their measured values in a shaded light line in reference Antenna 1. The computed code multipath closely follows the measured multipath errors. This was done for each visible satellite and for each reference antenna.

The effectiveness of the technique to remove multipath was assessed in two ways, namely in the measurement domain and in the position domain. The measurement domain approach will first be discussed. The code multipath error was derived by using the well-known code minus carrier technique whereby the ionospheric error was removed by a second order polynomial curve fit (Braasch, 1994). The estimated multipath from the multi-antenna assembly was then compared with the derived code minus carrier multipath to generate residuals and measurement domain statistics.

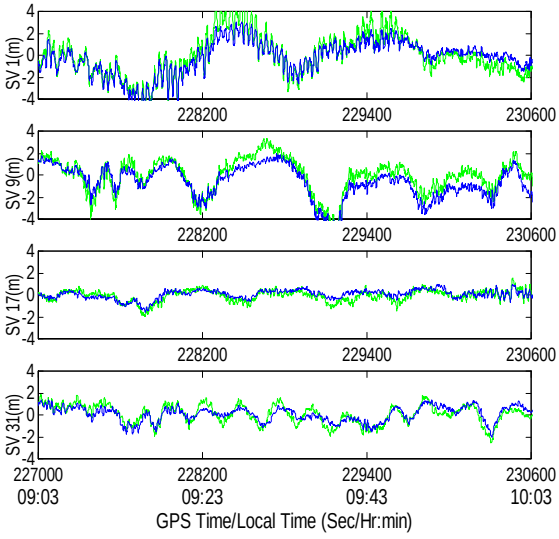

Figure 14: Measured multipath (light shade) and estimated multipath (dark shade) for SVs 1, 9, 17 and 31 at reference antenna 0.

Figure 15 shows the residuals for low elevation satellites in Antenna 1 with and without multipath correction. It is clear that the multipath-corrected residuals have smaller magnitudes compared to the uncorrected residuals.

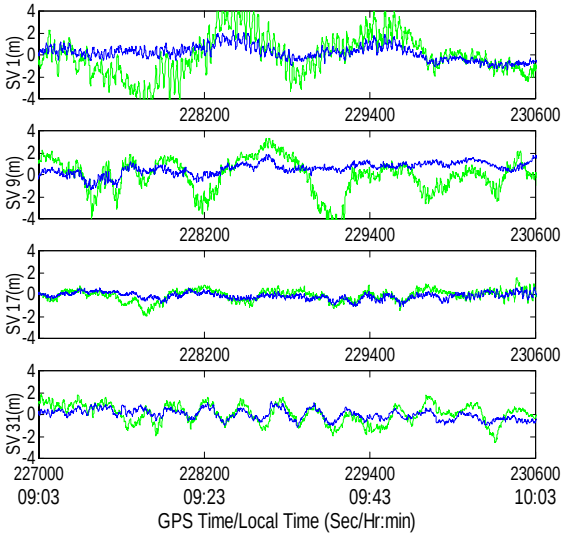

Figure 15: Code residuals before (light shade) and after (dark line) multipath correction for SVs 1, 9, 17 and 31 at reference antenna 0.

Table 1 gives the residual statistics before and after correction for low elevation satellites. It can be observed that this method is very effective in a high multipath environment decreasing the magnitude of the residuals up

to 65%. However, if the residuals are quite small before correction, the improvement is not significant.

Table 1: Code minus carrier and ionospheric delay compensated residuals before and after multipath correction

SV No. (Elv)	Ant. No.	Before Correction (m)	After Correction (m)	Improve-ment(%)
1 (14°-42°)	A0	1.89	0.66	64.96
	A1	0.54	0.62	-15.65
	A2	0.99	0.71	28.57
	A3	0.48	0.56	-17.65
	A4	0.66	0.76	-15.38
9 (13°-27°)	A0	1.56	0.54	65.46
	A1	0.90	0.52	41.65
	A2	0.58	0.61	-4.62
	A3	0.58	0.65	-12.66
	A4	0.72	0.62	13.96
17 (48°-21°)	A0	0.52	0.31	40.43
	A1	0.95	0.48	49.32
	A2	0.50	0.44	12.60
	A3	0.55	0.34	37.05
	A4	0.56	0.51	10.10
31 (23°-35°)	A0	0.85	0.47	45.08
	A1	0.76	0.55	27.48
	A2	0.88	0.97	-9.72
	A3	1.57	0.55	65.15
	A4	0.61	0.49	19.07

The second approach for assessing the effectiveness of the approach was in the position domain. The estimated multipath was removed from the raw reference receiver code data and DGPS positions of a pre-surveyed user 500 m away were computed. No multipath corrections were made at the user end, however the receiver was situated in an open field so it was assumed that the multipath effect would be minimal. The University of Calgary's C^{3}NAV^{TM} software (Cannon and Lachapelle, 1997) was used to compute DGPS positions with, and without, carrier smoothing. Position accuracies were computed for the smoothing versus no smoothing cases, as well as for the multipath correction versus no correction cases and appropriate statistics were generated.

Figure 16 shows the position error of the user with respect to reference Antenna 1 using a shaded light line. The user position was recomputed using multipath-corrected code measurements and the corresponding errors are shown in the same figure using a shaded dark line. It can be observed that the position errors with the corrected measurements have a smaller magnitude. This was also done with carrier smoothed code data, using a smoothing time of 100 to 200 seconds. A similar improvement in the position accuracy was observed after multipath correction.

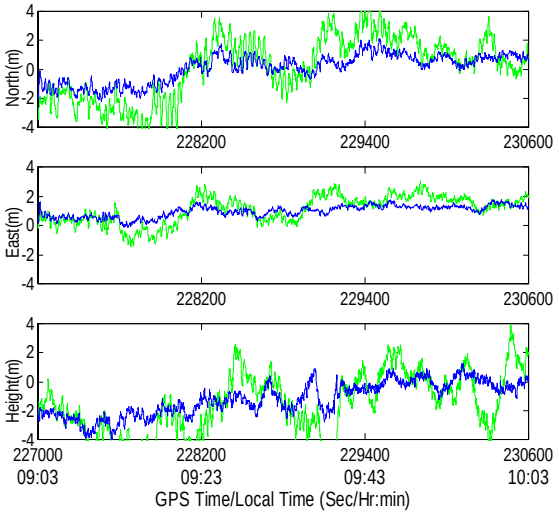

Figure 16: User position error using antenna 1 as reference antenna before (light shade) and after (dark shade) code multipath correction.

Table 2a: User position error without carrier-smooth code before and after multipath correction

Ant No.		σ_{before} (m)	σ_{after} (m)	Improve-ment (%)	Improve-ment (%)
A0	Lat	2.11	0.96	54.33	51.60
	Lon	0.93	0.39	58.02	
	Hgt	2.22	1.15	48.28	
A1	Lat	1.04	0.85	18.61	31.16
	Lon	0.67	0.40	39.93	
	Hgt	1.46	0.92	36.60	
A2	Lat	1.01	0.82	18.54	7.97
	Lon	0.54	0.56	-2.69	
	Hgt	1.34	1.28	4.27	
A3	Lat	1.01	0.73	27.86	40.35
	Lon	0.67	0.33	50.05	
	Hgt	1.61	0.90	44.38	
A4	Lat	0.60	0.72	-20.79	-3.68
	Lon	0.42	0.55	-30.41	
	Hgt	1.19	1.13	5.17	

The analysis was repeated using each of the reference antennas and the statistics are shown in Table 2a and 2b corresponding to the non-smoothed code and carrier smoothed code cases. Up to a 55% improvement in the 3D position position accuracy was achieved using this technique in both cases. Antenna 4 shows a negative improvement as the residuals slightly deteriorated in this case (although the absolute error is quite small).

Table 2b: User position error without carrier-smooth code before and after multipath correction

Ant No.		σ_{before} (m)	σ_{after} (m)	Improve-ment (%)	Improve-ment (%)
A0	Lat	2.11	0.96	54.33	51.60
	Lon	0.93	0.39	58.02	
	Hgt	2.22	1.15	48.28	
A1	Lat	1.04	0.85	18.61	31.16
	Lon	0.67	0.40	39.93	
	Hgt	1.46	0.92	36.60	
A2	Lat	1.01	0.82	18.54	7.97
	Lon	0.54	0.56	-2.69	
	Hgt	1.34	1.28	4.27	
A3	Lat	1.01	0.73	27.86	40.35
	Lon	0.67	0.33	50.05	
	Hgt	1.61	0.90	44.38	
A4	Lat	0.60	0.72	-20.79	-3.68
	Lon	0.42	0.55	-30.41	
	Hgt	1.19	1.13	5.17	

Carrier multipath error estimation from carrier measurements using the same set of data was done (Ray, 1999) and is not repeated here.

These results demonstrate that significant improvement in residuals and user position accuracy can be achieved by using such a multi-antenna system as reference station.

CONCLUSIONS

A technique has been developed and described to reduce the effect of multipath on code and carrier using a multi-antenna system. Tests were carried out at the University of Calgary using a multi-antenna assembly consisting of five closely-spaced antennas. NovAtel BeeLine™ receivers driven by a common oscillator were used for the experiment.

A comprehensive analysis of GPS receiver code and carrier tracking loop discriminator functions in the presence of multipath was carried out to characterize the behavior and formulate the errors in terms of multipath parameters. The SNR in the receiver was also related to the same parameters. The technique exploits the spatial correlation of multipath along with the known geometry among the antennas to estimate the multipath parameters. The multipath error for each satellite at each antenna was then estimated and removed from the raw measurements. Residuals, with and without multipath correction, were obtained and a comparison of residual statistics showed that the technique is effective in a high multipath environment reducing its effect up to 65% in the user receiver. The user position accuracy was also improved up to 55% by using this technique.

One of the limitations of this technique was that the formulation did not support code multipath from far away reflectors. Further investigations are to be made to overcome this deficiency.

ACKNOWLEDGEMENTS

Thanks to Waldemar Kunysz of NovAtel Inc. for technical support and logistics. One of the first authors (J.K.R) thanks University Technologies International Inc. and the Canadian Institute of Geomatics for their financial support during his graduate program.

REFERENCES

Axelrad, P., C.J. Comp, and P.F. MacDoran (1996), SNR Based Multipath Error Correction for GPS Differential Phase, IEEE Transactions on Aerospace & Electronic Systems, Vol. 32, No. 2, April, 650-660.

Bartone, C. and Frank van Graas (1998), Airport Pseudolites for Local Area Augmentation, Proceedings of IEEE PLANS, Catalogue No. 98CH36153, Palm Springs, April 20-23, pp. 479-486.

Braasch M.S. (1994), Isolation of GPS Multipath and Receiver Tracking Errors, Proceedings of ION National Technical Meeting, San Diego, pp. 511-521.

Braasch, M.S. (1996), Multipath Effects, Global Positioning Systems: Theory and Applications, American Institute of Aeronautics and Astronautics, Vol. 1, Chapter 14, pp. 547-568.

Cannon, M.E. (1993), SEMIKIN™ Operating Manual, Version 2.0, Department of Geomatics Engineering, The University of Calgary, Calgary, AB. Canada. 12 pp.

Cannon, M.E. and G. Lachapelle (1997), C^{3}NAV Operating Manual, Ver 1.3, The University of Calgary, 17 pp.

Counselman, C.C. (1998), Array Antennas for DGPS, Proceedings of IEEE PLANS, Palm Springs, April 20-23, 1998, pp. 352-357.

Decleene, B., T. Murphy and T. A. Skidmore (1997), Specifics of LAAS Context Model (G(x)), Proceedings of ION GPS-97, Kansas City, September 16-19, pp. 1583-1592.

Ford, T., W. Kunysz, R. Morris, J. Neumann, J. Rooney and T. Smit (1997), Beeline RT20-a Compact, Medium Precision Positioning System with and Attitude, Proceedings of ION GPS-97, Kansas City, pp. 687-695.

Garin, L., F. van Diggelen and J. Rousseau (1996), Strobe & Edge Correlator Multipath Mitigation for Code, Proceedings of ION GPS-96, Kansas City, September 17-20, pp. 657-664.

Garin L and J. Rousseau (1997), Enhanced Strobe Correlator Multipath Rejection for Code & Carrier, Proceedings of ION GPS-97, September 16-19, Kansas City, pp. 559-568.

GEC Plessey Semiconductors (1996), Advance information on GP2021, GPS 12 channel correlator with microprocessor support function, July, 60 pp.

Gelb, A. (1979), Applied Optimal Estimation, MIT Press, Massachusetts Institute of Technology, Massachusetts, Cambridge, 374 pp.

Hatch, R. (1982), The Synergism of GPS Code and Carrier Measurement. Proceedings of Third International Geodetic Symposium on Satellite Doppler Positioning, DMA/NGS, Washington, D.C., pp. 1213-1232.

Lachapelle, G. (1997), Lecture notes of GPS Theory and applications, The University of Calgary, Fall 1997, 444 pp.

Maybeck, P.S. (1994), Stochastic Models, Estimation, and Control, Vol. 1, Navtech, Arlington, 423 pp.

Ray, J.K., M.E. Cannon and P. Fenton (1998), Mitigation of Static Carrier Phase Multipath Effects Using Multiple Closely-Spaced Antennas, Proceedings of ION GPS-98, Nashville, September 15-18, pp. 1025-1034.

Ray, J.K. and M.E. Cannon (1999), Characterization of GPS Carrier Phase Multipath, Proceedings of ION NTM-99, San Diego, January 25-27, pp. 343-352.

Ray, J.K. (1999), Use of multiple antennas to mitigate carrier phase multipath in reference stations, Proceedings of ION GPS-99, Nashville, September 14-17, (in press).

Spilker Jr., J. J. (1996), GPS Signal Structure and Theoretical Performance, Chapter 2, Global Positioning Systems: Theory and Applications, American Institute of Aeronautics and Astronautics, Vol. 1, Chapter 3, pp. 57-120.

Townsend, B. and P. Fenton (1994), A Practical Approach to the Reduction of Pseudorange Multipath Errors in a L1 GPS Receiver, Proceedings of ION GPS-94, Salt Lake City, September 20-23, pp. 143-148.

Townsend, B., P. Fenton, K.van Dierendonck and R.D.J. van Nee (1995), L1 Carrier Phase Multipath Error Reduction Using MEDLL Technology, Proceedings of ION GPS-95, Palm Spring, September 12-15, pp. 1539-1544.

van Dierendonck, A.J., P. Fenton and T. Ford (1992), Theory and Performance of Narrow Correlator Technology in GPS Receiver, NAVIGATION: Journal of The Institute of Navigation, Vol. 39, No. 3, pp. 265-283.

van Nee, R.D.J. (1995), Multipath and Multi-Transmitter Interference in Spread-Spectrum Communication and Navigation Systems, Delft University Press, Delft, The Netherlands, 208 pp.

Ward, P. (1996), Satellite Signal Acquisition and Tracking, Chapter 5, Understanding GPS Principles and Applications, Editor: E. D. Kaplan, Artech House, Boston, pp. 119-208.